Research Square

Preprints are preliminary reports that have not undergone peer review.
They should not be considered conclusive, used to inform clinical practice,
or referenced by the media as validated information.

Metabolomic Profiling and Putative Identification of Bioactive Compounds from *Zymomonas mobilis* Exhibiting Antibacterial and Antidiabetic Properties

Kozhir Karim Abdalla
Pukyong National University
Jun Ho Yim
Pukyong National University
Seong Seok Choi
Pukyong National University
Naz Kamaran Ahmed
Pukyong National University
Min Jae Kang
Pukyong National University
Yong Tae Jeong
Nakdonggang National Institute of Biological Resources
Jae Sung Yun
University of Surrey
Buyng Su Hwang
Nakdonggang National Institute of Biological Resources
Young Jae Jeon
youngjaejeon@pknu.ac.kr
Pukyong National University

Research Article

Keywords: Zymomonas mobilis, multidrug resistance, antidiabetic activity, bioassay-guided fractionation, diketopiperazines, cyclo(Pro–Leu)

Posted Date: July 10th, 2026

DOI: https://doi.org/10.21203/rs.3.rs-10209588/v1

License: This work is licensed under a Creative Commons Attribution 4.0 International License. Read Full License

Additional Declarations: No competing interests reported.

Abstract

Background *Zymomonas mobilis* is traditionally recognized for its industrial ethanol production; however, it has recently gained attention as a potential source of bioactive secondary metabolites. This study aimed to evaluate the antibacterial and antidiabetic potential of crude extracts from different *Z. mobilis* strains and to explore their metabolomic and genomic characteristics.

Methods Crude extracts from three *Z. mobilis* strains (ZM4, ZM401, and ZM6) were evaluated by disk diffusion after liquid–liquid extraction/fractionation. The active peaks were separated by high-performance liquid chromatography (HPLC), and the active fractions were analyzed by gas chromatography–mass spectrometry (GC–MS) for compound identification. In silico genomic analysis of the reference strain ZM4 was conducted to investigate the presence of biosynthetic gene clusters. Antidiabetic activity was assessed by measuring glucose uptake in dexamethasone-induced insulin-resistant L6 myotubes.

Results Among the tested strains, ZM6 exhibited the strongest antibacterial activity, particularly against MDR *Escherichia coli* and *Klebsiella pneumoniae*. GC–MS analysis of the n-butanol fraction revealed the presence of diketopiperazines, predominantly cyclo(Pro–Leu) (up to 56.02%), along with β-carboline compounds. Genomic analysis showed the absence of canonical biosynthetic gene clusters, including cyclodipeptide synthases and non-ribosomal peptide synthetases, suggesting the involvement of alternative or uncharacterized biosynthetic pathways. Additionally, the ZM6 aqueous crude extract significantly enhanced glucose uptake in insulin-resistant L6 myotubes, reaching approximately 20 mM, which was associated with the detection of D-allose-rich fractions (44.28%).

Conclusions These findings demonstrate that *Z. mobilis*, particularly strain ZM6, is a promising source of bioactive metabolites with antibacterial activity against MDR pathogens and potential antidiabetic effects. The discrepancy between metabolite production and genomic predictions suggests the existence of unexplored biosynthetic mechanisms that warrant further biochemical and genomic investigation.

Introduction

Zymomonas mobilis is a Gram-negative facultative anaerobic bacterium well known for its exceptionally high ethanol productivity driven by the energy-efficient Entner-Doudoroff (ED) pathway. This pathway generates one mole of ATP per mole of glucose and supports near-theoretical ethanol yield (up to 98%), combined with rapid glucose uptake rates, making *Z. mobilis* a valuable industrial microorganism for bioethanol production [1, 2]. *Z. mobilis* also exhibits strong tolerance to harsh fermentation conditions, including high sugar concentrations (up to 400 g L^{-1}) and elevated ethanol levels (up to 160 g L^{-1}), further enhancing its suitability for industrial bioprocesses [3, 4, 5].

Importantly, *Zymomonas mobilis* is generally recognized as safe (GRAS), enabling its application beyond biofuel production in food-related fields. Previous studies have demonstrated that *Z. mobilis* can produce fructooligosaccharides (FOSs), well-established prebiotic compounds known to selectively stimulate beneficial gut microbiota. Consumption of FOSs produced by *Z. mobilis* has been associated with reduced cholesterol and blood lipid levels in both clinical and animal studies [6, 7]. Metabolic engineering studies have further expanded the biosynthetic capacity of *Z. mobilis* for the production of value-added compounds such as pyruvate, succinic acid, and lactic acid, underscoring its versatility as a microbial cell factory [8–14].

Beyond its industrial relevance, *Z. mobilis* has attracted growing interest due to its diverse biological activities. Several studies have reported the production of metabolites exhibiting antibacterial, antitumor, and antiparasitic effects, including bacteriocins, levans, and peroxide-related metabolites [15, 16, 17]. Specifically, inhibitory effects against *Schistosoma mansoni* infections and antitumor activity against Sarcoma 180 have been documented [18, 19, 20].

Despite these findings, the specific mechanisms and compounds underlying the antibacterial activity of *Z. mobilis* remain partially characterized. Bacteriocins produced by Zymomonas mobilis Z1-87 have been suggested to contribute to broad-spectrum antibacterial activity against human pathogens [17]. In contrast, antibacterial effects observed in Z. mobilis strains ZM4 and ZM6 have been primarily attributed to acidic metabolic byproducts, such as acetate and propionate, generated under aerobic conditions [21]. These contrasting interpretations highlight a critical knowledge gap regarding the nature of the antibacterial compounds produced by *Z. mobilis*, particularly under non-aerobic cultivation conditions where organic acid production may differ. Furthermore, while the antibacterial potential has been debated, comparatively little attention has been paid to the potential antidiabetic properties of *Z. mobilis*-derived secondary metabolites, limiting our understanding of its broader therapeutic potential.

Thus, this study aimed to systematically evaluate the antibacterial and antidiabetic activities of *Z. mobilis* strains (ZM4, ZM401, and ZM6) to address these gaps in the context of the increasing global concern of multidrug-resistant (MDR) bacterial infections and metabolic disorders. Unlike previous studies focusing on acidic byproducts or proteinaceous bacteriocins, we employed a bioassay-guided fractionation approach coupled with gas chromatography-mass spectrometry (GC-MS) analysis to identify specific bioactive small molecules. By linking the observed therapeutic phenotypes, specifically inhibition of MDR pathogens and enhanced glucose uptake, to distinct metabolic profiles, this work provides new insights into the potential of *Z. mobilis* as a microbial platform for producing bioactive metabolites with therapeutic potential.

Materials and Methods

Bacterial strains and cultivation

All *Zymomonas mobilis* strains (ZM4, ATCC 31821; ZM401, ATCC 31822; and ZM6, ATCC 29191) were cultivated for 48 h at 30°C under stationary conditions in Rich Medium (RM) broth [22]. The medium contained 20 g L^{-1} D-glucose (98%, Junsei Chemical Co., Tokyo, Japan), 10 g L^{-1} yeast extract (food microbiological grade, Cellconic, Seoul, Republic of Korea), 2 g L^{-1} potassium phosphate monobasic (99%, Sigma-Aldrich, St. Louis, MO, USA), 1 g L^{-1} magnesium sulfate anhydrous (99.5%, Shinyo Chemical Co., Ltd., Republic of Korea), and 1 g L^{-1} ammonium sulfate (extra pure, Samchun Chemical Co., Ltd.,

Republic of Korea), with the pH adjusted to 6.5. Glucose was autoclaved separately to prevent thermal degradation. Fourteen pathogenic bacterial strains were used as indicator strains for antibacterial assays. Five *Vibrio* species were cultivated on trypticase soy agar (Becton, Dickinson and Company, Franklin Lakes, NJ, USA), while MDR *Escherichia coli* and *Klebsiella pneumoniae* were cultivated on nutrient agar (Becton, Dickinson and Company) [23]. All indicator strains used in this study are listed in Table 1.

Table 1
Disk diffusion assay indicator strains of *Z. mobilis* against gram-positive and gram-negative pathogens.

Gram's stain	Bacterial pathogens	Strains
Gram-negative	*Vibrio parahaemolyticus*	KCCM 11965
	Vibrio anguillarum	KCTC 2711
	Vibrio damsela	JF21023NE
	Vibrio harveyi	Vh21fl
	Vibrio scophthalmi	JF21004NE
	Pseudomonas aeruginosa	ATCC 27853
	Escherichia coli multidrug-resistant	CPEc171209
	Escherichia coli	ATCC 25922
	Klebsiella pneumoniae	ATCC BAA-2146
	Klebsiella pneumoniae	ATCC BAA-1706
	Klebsiella pneumoniae multidrug-resistant	CPKp171210
Gram-positive	*Enterococcus faecalis*	ATCC 29212
	Staphylococcus aureus	ATCC 29213
	Bacillus subtilis	KCCM 11779

Fermentation and extractions

Seed cultures were prepared by inoculating a single colony of each *Z. mobilis* strain into 200 mL of RM broth and incubating at 30°C until reaching an optical density (OD) at 660 nm of approximately 1.0. The seed culture (10% v/v) was then inoculated into 1.5 L of fresh RM broth and fermented for 48 h under stationary conditions. The cell-free supernatant was obtained by centrifugation (9000 rpm, 5 min) and filtration using 0.20 µm syringe filters (SFCA03022, SOOMBIO, Republic of Korea) to remove any remaining particulate matter. The supernatant was sequentially extracted with hexane (99%, Duksan, Ansan, Republic of Korea), ethyl acetate (99.7%, Samchun Chemical Co., Ltd., Republic of Korea), and n-butanol (99%, Duksan, Ansan, Republic of Korea) at a supernatant-to-solvent ratio of 1:2 (v/v). After each extraction step, the organic phase was separated, and the remaining aqueous phase was subjected to extraction with the next solvent. The organic layers were concentrated using a rotary evaporator (Ev-1001V Diagonal type, Scilab, Republic of Korea) at 45°C and lyophilized for 72 h at -76°C using a freeze-dryer (FDU-2200, Eyela, Republic of Korea) to obtain dried crude extracts. All glassware used for extraction was acid-cleaned prior to use to eliminate potential contaminants [24].

Antibacterial susceptibility assays

The antibacterial activity of the crude extracts was evaluated using a modified Kirby-Bauer disk diffusion method [25]. Bacterial suspensions were adjusted to the 0.5 McFarland standard (approximately 1 x 10^8 CFU mL^{-1}) [26]. Paper disks (6.5 mm, Advantec, Tokyo, Japan) were loaded with 20 µL of each crude extract (5 mg mL^{-1}), which had been dissolved in distilled water prior to use. All treatments, including positive and negative controls, were applied in an equal volume of 20 µL per disk. Enrofloxacin (99.0%, Sigma-Aldrich; 50 µg mL^{-1}) was used as the positive control, and 1× phosphate-buffered saline (PBS; Bylabs, Republic of Korea) served as the negative control. The inhibition zones were measured after incubation at 37°C for 24 h.

High-performance liquid chromatography fractionation

Crude extracts were fractionated using a Waters Alliance 2695 HPLC system (Waters, Milford, MA, USA) following a modified protocol [27]. Chromatographic separation was conducted on a SunFire C_8 column (4.6 × 250 mm, 5 µm; Waters). The mobile phases consisted of 0.1% formic acid in water (solvent A) and 0.1% formic acid in acetonitrile (solvent B). Isocratic elution was performed with 95% solvent A and 5% solvent B at a flow rate of 0.7 mL min^{-1}. The injection volume was 50 µL, and the column temperature was maintained at 25°C. Fractions corresponding to each chromatographic peak were collected from 60 repeated injections and pooled to obtain sufficient material for downstream analyses. The collected fractions were subsequently freeze-dried.

Antibacterial screening of high-performance liquid chromatography fractions

The dried HPLC fractions were dissolved in distilled water prior to screening and evaluated for antibacterial activity against *Vibrio parahaemolyticus* using a 96-well plate assay. Each well contained 50 µL of bacterial suspension (1.5×10^8 CFU mL^{-1} in tryptic soy broth) and 50 µL of each resuspended fraction. Enrofloxacin (50 µg mL^{-1}, 50 µL per well) was used as the positive control. After incubation at 20°C for 24 h, bacterial growth was assessed by measuring turbidity to identify active fractions.

GC-MS identification of bioactive compounds

Active HPLC fractions were analyzed using a Shimadzu GC-MS QP-2010 Ultra system (Shimadzu, Kyoto, Japan) equipped with a DB-5MS Ultra capillary column (30 m × 0.25 mm, 0.25 µm film thickness) [28]. Samples were prepared by dissolving dried fractions in HPLC-grade methanol (300 µL). A 1.0 µL aliquot was injected in split mode (50:1) at an injection temperature of 280°C. The oven temperature was programmed from 60°C to 200°C (10°C min^{-1}) and then to 320°C (20°C min^{-1}). Helium (99.9%) was used as the carrier gas at 1.0 mL min^{-1}. Compounds were tentatively identified by matching electron impact (EI) mass spectra against the NIST 17 library, using a similarity index threshold of > 90%. The five best matches ranked by similarity index were considered for compound annotation. The system operated at 70 eV, generating characteristic fragmentation patterns.

Semi-quantitative analysis of bioactive compounds

A semi-quantitative analysis based on GC-MS total ion chromatograms (TIC) was performed to evaluate the relative composition of the identified bioactive compounds. The relative abundance (%) of each compound was calculated using the following equation:

$$\text{Relative abundance } (\%) = \left(\frac{\text{peak area of individual compound}}{\text{total peak area}} \right) \times \ 100$$

This approach identified major constituents contributing to the observed antibacterial and antidiabetic activities.

Cell culture and cytotoxicity assay

L6 rat myoblasts (ATCC CRL-1458) were obtained from the American Type Culture Collection (ATCC, Manassas, VA, USA). Cells were maintained in Dulbecco's Modified Eagle Medium (DMEM, Corning, NY, USA)) supplemented with 10% heat-inactivated fetal bovine serum (FBS, Corning, NY, USA)) and 1% penicillin-streptomycin solution at 37°C in a humidified atmosphere containing 5% CO_2. Differentiation was induced by switching the medium to DMEM supplemented with 2% FBS for 7 days. Cytotoxicity was evaluated using the WST-1 assay [29]. Differentiated L6 cells were treated with crude extracts at concentrations of 100, 200, and 400 µg mL^{-1} for 24 h. Cell viability was determined by measuring absorbance at 450 nm using an EZ-Cytox Cell Viability Assay Kit (DoGenBio, Seoul, Republic of Korea) according to the manufacturer's instructions.

Glucose consumption assay

Glucose uptake was assessed in differentiated L6 myotubes divided into three groups: differentiated-only control (D.O.), insulin-stimulated control (Ins), and dexamethasone-induced insulin-resistant group (Dex). Insulin resistance was induced by treating cells with 0.25 µM dexamethasone for 24 h prior to treatment. The culture medium was replaced with serum-free DMEM to eliminate serum interference. Cells were then treated with crude extracts (400 µg mL^{-1}) for 24 h. For Ins and Dex groups, 100 nM insulin was co-administered during treatment. Residual glucose in the medium was measured using a Glucose Colorimetric Assay Kit (E-BC-K234-S, Elabscience, Houston, TX, USA), and glucose consumption was calculated accordingly.

In silico analysis

Genes involved in the biosynthesis of secondary metabolites were identified using bioinformatic tools, including BLAST, UniProt, PRISM, and antiSMASH, to analyze potential biosynthetic gene clusters.

Statistical analysis

Statistical analyses were performed using GraphPad Prism 8 (GraphPad Software, San Diego, CA, USA). Data are presented as mean ± standard deviation (SD). Differences among groups were analyzed using two-way ANOVA followed by Tukey's post-hoc test. Statistical significance was considered at $p < 0.05$.

Results

Antibacterial activity and strain-dependent profiles of Z. mobilis crude extracts

To evaluate the antibacterial activity of crude extracts from *Z. mobilis* strains (ZM4, ZM401, and ZM6), a disk diffusion assay was performed, as shown in the heatmap in Fig. 1. Antibacterial activity varied depending on both the extraction solvent and the producing strain. The hexane and ethyl acetate fractions showed no detectable antibacterial activity against any of the tested indicator strains. In contrast, the n-butanol fractions exhibited inhibitory effects against multiple bacterial strains.

Among the tested strains, ZM6 showed the highest antibacterial activity. The n-butanol extract of ZM6 produced inhibition zones of 14.0 mm against *Staphylococcus aureus* and 12.7 mm against *Vibrio anguillarum*. Notably, inhibitory activity was also observed against multidrug-resistant (MDR) *Klebsiella pneumoniae* and *Escherichia coli*, with inhibition zones ranging from 6.5 to 8.0 mm. In contrast, no inhibition zones were observed for these MDR strains in the presence of enrofloxacin under the tested disk diffusion conditions.

Regarding the water-phase crude extracts, strain-dependent differences were observed. Overall, the water-phase extracts showed no detectable activity against Gram-positive bacteria or MDR strains. However, weak inhibitory activity was observed against several *Vibrio* species, with inhibition zones ranging from 6.8 to 9.0 mm.

Chromatographic profiles and fractionation

All crude extracts (n-butanol and water-phase fractions) were subjected to high-performance liquid chromatography (HPLC) to separate individual fractions for subsequent antibacterial screening. Fraction activity was evaluated against *Vibrio parahaemolyticus*, which was selected as a representative indicator strain due to its consistent susceptibility to both n-butanol and water-phase extracts. The detailed fractionation profiles, relative abundance of major peaks, and antibacterial screening results for the water-phase extracts are summarized in Table 2, while those for the n-butanol extracts are presented in Table 3.

Table 2
HPLC fractionation profile, relative abundance, and antibacterial screening results of water-phase crude extracts from *Z. mobilis* strains.

Strain	Peak ID (Fig. 2)	Retention time (min)	HPLC relative peak area (%) [a]	Antibacterial activity [b]	Major compound identified (by GC-MS)	GC-MS relative abundance (%) [c]
ZM6	WP1	3.6	57.43	+++	α-Amino-Ɛ-caprolactam	58.95
					Cyclo (Pro-Leu)	6.27
					Cyclo (Pro-Phe)	3.72
	WP2	5.1	22.65	++	1,2,3-Propanetriol	38.75
					5-Oxoproline methyl ester	5.80
					Cyclo (Val-Ala)	3.85
	WP3	5.3	6.09	++	D-Allose	27.82
					1,2,3-Propanetriol	27.07
					5-Oxoproline methyl ester	6.70
	WP4	5.5	5.79	++	D-Allose	44.28
					1,2,3-Propanetriol	10.71
					2-Pyrrolidinone	4.53
	WP5	5.8	3.68	++	D-Allose	31.77
					1,2,3-Propanetriol	10.45
					2-Methyl-N-(2-methylbutylidene) butan-1-amine	6.69
	WP6	6.3	4.37	+++	2-Methyl-N-(2-methylbutylidene) butan-1-amine	56.62
					D-Allose	11.09
					1,2,3-Propanetriol	2.46
ZM401	WP1	3.6	59.28	-	1,6-anhydro-*β*-D-glucopyranose,	12.68
					1,4:3,6-dianhydro-α-D-glucopyranose	2.46
					1,2,3-Propanetriol	2.08
	WP2	5.1	23.03	++	1,2,3-Propanetriol	31.38
					2-Pyrrolidinone	11.08
					D-Alanine	5.73
	WP3	5.6	6.08	++	D-Allose	41.65
					1,2,3-Propanetriol	22.69
					1,6-Anhydro-α -D-galactofuranose	4.64
	WP4	5.9	5.87	++	D-Allose	37.66
					1,2,3-Propanetriol	4.63
					Levoglucosenone	4.18
	WP5	6.4	5.74	++	α-Amino-Ɛ-caprolactam	29.40
					Cyclo (Pro-Phe)	8.73
					Cyclo (Pro-Leu)	7.08

[a]Relative fraction area (%): calculated from the HPLC chromatogram (Fig. 2) at 210 nm, representing the proportion of each fraction within the crude extract.

[b]Antibacterial activity was assessed qualitatively by the visual observation of turbidity in 96-well plates compared to untreated negative controls: (+++) indicates strong/complete growth inhibition (clear well); (+) indicates partial growth inhibition (noticeably reduced turbidity); (-) indicates no inhibition (dense growth equivalent to the control).

[C]GC-MS relative abundance (%): calculated based on the gas chromatography-mass spectroscopy (GC-MS) total ion chromatogram described in Section 2.8, representing the proportion of the specific compound within the fraction.

Strain	Peak ID (Fig. 2)	Retention time (min)	HPLC relative peak area (%) [a]	Antibacterial activity [b]	Major compound identified (by GC-MS)	GC-MS relative abundance (%) [c]
ZM4	WP1	3.6	66.67	-	α-Amino-ε-caprolactam	26.33
					Cyclo (Pro-Phe)	11.72
					Cyclo (Pro-Leu)	11.42
	WP2-1	4.9	13.62	-	2-Pyrrolidinone	31.41
					5-oxoproline methyl ester	13.85
					α-Amino-ε-caprolactam	8.88
	WP2-2	5.1	8.96	++	1,2,3-Propanetriol	48.77
					Cyclo (Pro-Gly)	3.18
					Octadecanoic acid	2.48
	WP3	5.2	4.49	++	1,2,3-Propanetriol	46.73
					D-Allose	10
					Cyclo (Val-Val)	2.15
	WP4	6.2	6.27	++	2-Methyl-N-(2-methylbutylidene) butan-1-amine	35
					D-Allose	13.12
					1,2,3-Propanetriol	5.29

[a]Relative fraction area (%): calculated from the HPLC chromatogram (Fig. 2) at 210 nm, representing the proportion of each fraction within the crude extract.

[b]Antibacterial activity was assessed qualitatively by the visual observation of turbidity in 96-well plates compared to untreated negative controls: (+++) indicates strong/complete growth inhibition (clear well); (+) indicates partial growth inhibition (noticeably reduced turbidity); (-) indicates no inhibition (dense growth equivalent to the control).

[C]GC-MS relative abundance (%): calculated based on the gas chromatography-mass spectroscopy (GC-MS) total ion chromatogram described in Section 2.8, representing the proportion of the specific compound within the fraction.

Table 3
HPLC fractionation profile, relative abundance, and identification of bioactive compounds in the *n*-butanol extract of *Z. mobilis* strains.

Strain	Peak ID (Fig. 3)	HPLC retention time (min)	HPLC relative peak area (%) [a]	Antibacterial activity [b]	Major compound identified (by GC-MS)	GC-MS relative abundance (%) [c]
ZM6	BP1	3.3	3.30	++	Cyclo (Pro-Leu)	28.47
					Cyclo (Pro-Gly)	12.47
					Cyclo (Pro-Phe)	5.87
	BP2	3.6	2.61	+++	Cyclo (Pro-Leu)	56.02
					Benzeneacetic acid	12.68
					Cyclo (Pro-Phe)	2.31
	BP3	3.8	2.76	+++	Cyclo (Pro-Leu)	53.87
					Benzeneacetic acid	10.76
					Cyclo (Pro-Phe)	3.79
	BP4	4.0	1.40	-	(Z)-13-Docosenamide	17.49
					(Z)-9-Octadecenamide,	14.03
					2-Pyrrolidinone	9.27
	BP5	4.8	17.04	-	N-Ethylproline methyl ester	10.36
					(Z)-13-Docosenamide	9.22
					Benzeneacetic acid	2.22
	BP6	5.0	43.60	-	(Z)-13-Docosenamide	16.17
					Niacinamide	2.59
					Cyclo (Phe-Trp)	1.88
	BP7	5.9	10.79	-	(Z)-13-Docosenamide	9.88
					Tyramine	3.95
					Cyclo (Gly-Ala)	1.55
	BP8	6.2	6.71	-	(Z)-9-Octadecenamide,	14.65
					(Z)-13-Docosenamide	5.85
					Niacinamide	3.16
	BP9	6.5	3.72	-	2-Methyl-N-(2-methylbutylidene) butan-1-amine	22.05
					(Z)-13-Docosenamide	8.98
					(Z)-9-Octadecenamide,	2.12
	BP10	8.4	2.96	-	(Z)-9-Octadecenamide,	12.14
					(Z)-13-Docosenamide	7.64
					2-Pyrrolidinone	2.69
	BP11	8.9	5.10	++	Cyclo (Pro-Gly)	24.83
					Cyclo (Pro-Phe)	3.21
					9H-Pyrido[3,4-b] indole (*β*-carboline)	0.78
ZM401	BP1	3.1	1.69	-	(Z)-9-Octadecenamide,	28.52

[a]Relative fraction area (%): calculated from the integration of the HPLC chromatogram (Fig. 3), representing the abundance of the fraction in the extract.

[b]Antibacterial activity was assessed qualitatively by the visual observation of turbidity in 96-well plates compared to untreated negative controls: (+++) indicates strong/complete growth inhibition (clear well); (+) indicates partial growth inhibition (noticeably reduced turbidity); (-) indicates no inhibition (dense growth equivalent to the control).

[c]GC-MS relative abundance (%): calculated based on the gas chromatography-mass spectroscopy (GC-MS) total ion chromatogram described in Section 2.8, representing the proportion of the specific compound within the fraction.

Strain	Peak ID (Fig. 3)	HPLC retention time (min)	HPLC relative peak area (%) [a]	Antibacterial activity [b]	Major compound identified (by GC-MS)	GC-MS relative abundance (%) [c]
					(Z)-13-Docosenamide	15.54
					Hexadecanoic acid	4.45
	BP2	3.4	8.07	-	(Z)-9-Octadecenamide,	31.04
					(Z)-13-Docosenamide	21.05
					Hexadecanamide	4.16
	BP6-1	5.2	62.85	-	(Z)-13-Docosenamide	18.39
					(Z)-9-Octadecenamide,	6.83
					Hexadecanoic acid	5.17
	BP6-2	5.6	7.05	+	(Z)-13-Docosenamide	32.20
					Cyclo (Pro-Phe)	2.56
					9H-Pyrido[3,4-b] indole (β-carboline)	1
	BP7	5.9	10.38	-	(Z)-13-Docosenamide	13.59
					(Z)-9-Octadecenamide,	12.72
					Tyramine	3.98
	BP8	6.3	7.15	-	2-Methyl-N-(2-methylbutylidene) butan-1-amine	10.73
					(Z)-13-Docosenamide	6.69
					(Z)-9-Octadecenamide,	3.23
	BP9	6.6	2.81	-	(Z)-13-Docosenamide	10.42
					2-Methyl-N-(2-methylbutylidene) butan-1-amine	8.57
					(Z)-9-Octadecenamide,	4.43
ZM4	BP1	3.3	1.69		Cyclo (Pro-Gly)	8.69
				-	Cyclo (Pro-Leu)	7.68
					Tyrosol	2.74
	BP2	3.6	1.36		(Z)-13-Docosenamide	33.55
				-	Cyclo (Pro-Leu)	7.24
					Tyrosol	5.58
	BP3	3.9	3.76		(Z)-13-Docosenamide	36.12
				-	Cyclo (Pro-Leu)	7.71
					Tyrosol	4.79
	BP4	4.1	1.34		(Z)-9-Octadecenamide,	14.42
				-	Cyclo (Pro-Leu)	8.44
					(Z)-13-Docosenamide	3.70
	BP5	5.4	54.60		(Z)-13-Docosenamide	16.92
				-	Niacinamide	3.44

[a]Relative fraction area (%): calculated from the integration of the HPLC chromatogram (Fig. 3), representing the abundance of the fraction in the extract.

[b]Antibacterial activity was assessed qualitatively by the visual observation of turbidity in 96-well plates compared to untreated negative controls: (+++) indicates strong/complete growth inhibition (clear well); (+) indicates partial growth inhibition (noticeably reduced turbidity); (-) indicates no inhibition (dense growth equivalent to the control).

[C]GC-MS relative abundance (%): calculated based on the gas chromatography-mass spectroscopy (GC-MS) total ion chromatogram described in Section 2.8, representing the proportion of the specific compound within the fraction.

Strain	Peak ID (Fig. 3)	HPLC retention time (min)	HPLC relative peak area (%) [a]	Antibacterial activity [b]	Major compound identified (by GC-MS)	GC-MS relative abundance (%) [c]
					Cyclo (Phe-Trp)	0.92
	BP6	6.0	12.15		(Z)-13-Docosenamide	14.04
				-	Niacinamide	5.54
					Cyclo (Phe-Trp)	1
	BP7	6.4	10.86	-	2-Methyl-N-(2-methylbutylidene) butan-1-amine	17.93
					(Z)-9-Octadecenamide,	6.91
					(Z)-13-Docosenamide	5.32
	BP8	6.7	6.55	+	Cyclo (Pro-Leu)	11.48
					2-Methyl-N-(2-methylbutylidene) butan-1-amine	10.46
					9H-Pyrido[3,4-b] indole (*β*-carboline)	1.21
	BP9	9.2	7.70	+	Cyclo (Pro-Gly)	18.63
					(Z)-9-Octadecenamide,	8.94
					9H-Pyrido[3,4-b] indole (*β*-carboline)	0.74

[a]Relative fraction area (%): calculated from the integration of the HPLC chromatogram (Fig. 3), representing the abundance of the fraction in the extract.

[b]Antibacterial activity was assessed qualitatively by the visual observation of turbidity in 96-well plates compared to untreated negative controls: (+++) indicates strong/complete growth inhibition (clear well); (+) indicates partial growth inhibition (noticeably reduced turbidity); (-) indicates no inhibition (dense growth equivalent to the control).

[C]GC-MS relative abundance (%): calculated based on the gas chromatography-mass spectroscopy (GC-MS) total ion chromatogram described in Section 2.8, representing the proportion of the specific compound within the fraction.

Note: Ubiquitous lipophilic compounds such as 9-octadecenamide and (Z)-13-docosenamide formed a common background profile across multiple non-active fractions due to solvent partitioning.

The water-phase extracts exhibited a limited number of detectable chromatographic peaks across all strains, as shown in Fig. 2. In contrast, the n-butanol extracts displayed more complex chromatographic profiles with higher peak intensities, as illustrated in Fig. 3.

Major peaks from the water-phase extracts were designated as WP1–WP6, whereas peaks from the n-butanol extracts were designated as BP1–BP11. These fractions were collected over 60 repeated HPLC runs, lyophilized, and subsequently screened for antibacterial activity against *V. parahaemolyticus*. Among the tested strains, ZM6 exhibited the most prominent chromatographic peaks in the n-butanol fraction compared to ZM4 and ZM401. Fraction-level bioactivity data for all strains are provided in Supplementary Figures S1 and S2.

GC-MS identification of active fractions

All HPLC fractions were screened for antibacterial activity, and fractions exhibiting activity were further analyzed using gas chromatography–mass spectrometry (GC–MS) to characterize their chemical constituents.

In the water-phase extracts, antibacterial activity (+++) was observed primarily in ZM6-derived fractions. Fraction WP1 showed a high relative abundance of α-amino-ε-caprolactam (58.95%), whereas WP6 was dominated by Schiff base compounds, including 2-methyl-N-(2-methylbutylidene) butan-1-amine (56.62%). Diketopiperazine (DKP) derivatives, including cyclo(Pro-Leu) and cyclo(Pro-Phe), were also detected in WP1 at lower relative abundances. D-allose was detected across multiple fractions from all strains; however, its direct contribution to antibacterial activity could not be determined from GC–MS analysis alone.

In the n-butanol fractions, DKP derivatives were frequently detected in active fractions, particularly in ZM6. Fraction BP6 showed the highest relative abundance of (Z)-13-docosenamide (16.17%) but did not exhibit antibacterial activity. In contrast, strong antibacterial activity (+++) was observed in BP2 and BP3, where cyclo(Pro-Leu) was detected as a major component (56.02% and 53.87%, respectively). Fraction BP11 showed moderate activity (++) and contained cyclo(Pro-Gly) (24.83%), along with minor detection of 9H-pyrido[3,4-b]indole (β-carboline, 0.78%).

Antidiabetic potential of Z. mobilis extracts

The effect of *Z. mobilis* crude extracts on glucose uptake was evaluated in differentiated L6 myotubes under normal and dexamethasone-induced insulin-resistant conditions. Prior to the glucose uptake assay, cytotoxicity was assessed using a WST-1 assay. All crude extracts showed no significant cytotoxicity

at the tested concentration (400 μg mL^{-1}), with cell viability exceeding 95% in differentiated L6 myotubes. Under normal physiological conditions, treatment with crude extracts, either alone or in combination with insulin, did not significantly affect glucose consumption compared with controls (data not shown).

In contrast, under insulin-resistant conditions, treatment with *Z. mobilis* extracts significantly improved glucose consumption. The n-butanol crude extracts (400 μg mL^{-1}) induced a significant increase in glucose consumption (approximately 18–19 mM, $p < 0.05$) across all strains, as shown in Fig. 4A.

The water-phase extracts showed a more pronounced effect, as shown in Fig. 4B. Water-phase fractions from ZM4 and ZM401 significantly increased glucose consumption ($p < 0.05$) compared with the insulin-resistant control. Notably, the ZM6 water-phase extract exhibited the strongest effect, increasing glucose consumption to approximately 20.30 mM ($p < 0.001$) relative to the untreated dexamethasone-induced group.

In silico analysis of biosynthetic pathways

The genome of *Z. mobilis* ZM4 (NCBI accession No. NZ_CP023715.1) was analyzed using bioinformatic tools including BLAST, antiSMASH, and PRISM to explore potential biosynthetic gene clusters associated with metabolite production. Genes involved in central carbon metabolism were identified, including glycerol-3-phosphate dehydrogenase (GPD; ZMO1905). However, glycerol-3-phosphatase (GPP) was not annotated in the current genome dataset, despite the detection of glycerol-related metabolites in the experimental analysis. The Entner–Doudoroff (ED) pathway genes were confirmed and were consistent with the well-characterized metabolic framework of *Z. mobilis*.

Putative genes related to branched-chain amino acid metabolism, including aminotransferases, were identified; however, a complete set of enzymes required for canonical Ehrlich pathway conversion to higher alcohols and aldehydes was not fully resolved based on current genome annotation.

In addition, genome mining using the selected tools did not identify canonical cyclodipeptide synthases (CDPS), non-ribosomal peptide synthetases (NRPS), or tryptophan decarboxylase homologs that are typically associated with diketopiperazine or β-carboline biosynthesis. These observations suggest that the detected metabolites may be produced through alternative or currently uncharacterized biosynthetic routes in *Z. mobilis*.

Discussion

Based on the differential antibacterial activity observed across all solvent fractions, the results suggest that the bioactive compounds produced by *Z. mobilis* strains are influenced by solvent polarity. In particular, the absence of activity in hexane and ethyl acetate crude extracts, together with the strong activity observed in n-butanol crude extracts, indicates that the active antibacterial constituents are likely enriched in the semi-polar fraction [30]. The antibacterial activity of the ZM6 n-butanol extract, particularly against MDR *Klebsiella pneumoniae* and *Escherichia coli*, together with its activity pattern differing from that of enrofloxacin under the tested conditions, suggests the presence of bioactive compounds that may act through mechanisms distinct from those of conventional antibiotics.

In contrast, the antibacterial activity of water-phase crude extracts was mainly limited to *Vibrio* species, suggesting that hydrophilic compounds may exhibit a narrower antibacterial spectrum. This solvent-dependent distribution supports the idea that different classes of metabolites are partitioned according to polarity, with broader activity observed in semi-polar fractions. These findings differ from previous reports attributing the antibacterial activity of *Z. mobilis* primarily to bacteriocins or organic acids such as acetate and propionate. In the present study, solvent extraction combined with bioassay-guided fractionation suggests that the observed activity is associated with extractable small-molecule fractions rather than highly polar acids or macromolecular proteins.

GC–MS analysis of active fractions indicated that antibacterial activity in ZM6 crude extracts may be associated with nitrogen-containing metabolites, particularly diketopiperazines and heterocyclic compounds. However, due to the limitations of GC–MS-based identification, these associations should be interpreted cautiously and do not confirm direct causality.

In the water-phase crude extracts, antibacterial activity correlated with fractions enriched in α-amino-ε-caprolactam and Schiff base (imine) derivatives, which may plausibly originate from condensation reactions involving amino acid-derived degradation products potentially linked to Ehrlich-type pathways. These observations suggest that low-molecular-weight nitrogenous compounds may contribute to antibacterial effects in hydrophilic fractions. Aliphatic amines and imine derivatives have been reported to exhibit antimicrobial properties [14]. Their amphiphilic nature, involving protonatable nitrogen groups and hydrophobic alkyl chains, may enable interactions with bacterial membranes, potentially contributing to membrane perturbation and leakage of intracellular components [31]. The presence of diketopiperazines as minor components may indicate a supportive or secondary contribution to the overall activity rather than a dominant role in the active fractions. In addition, detection of D-allose across moderately active fractions may suggest a possible association with metabolically active fractions, although its direct functional role remains speculative.

Regarding the n-butanol-phase crude extracts, antibacterial activity did not show a clear correlation with total peak abundance. Instead, the frequent detection of diketopiperazine (DKP) derivatives, particularly cyclo (Pro-Leu), in the most active fractions suggests a potential association between these cyclic dipeptides and the observed antibacterial activity in *Z. mobilis* strains, especially ZM6. DKPs have been reported to exhibit antibacterial and antibiofilm activities, potentially through membrane interactions and modulation of cellular signaling processes [32, 33]. It should be noted that DKPs may also form artifactually during sample processing or GC–MS analysis through cyclization of dipeptides. However, their repeated detection across multiple bioactive fractions supports the possibility that they may represent genuine metabolites in addition to potential analytical artifacts. The detection of β-carboline compounds, although at low relative abundance, suggests that minor heterocyclic compounds may also contribute to antibacterial activity. β-carbolines have been reported to exhibit biological activities, including potential effects on bacterial efflux systems [34, 35].

The absence of a measurable effect under normal conditions suggests that *Z. mobilis* extracts do not significantly alter glucose metabolism under physiologically balanced conditions and do not excessively enhance basal insulin-responsive pathways. In contrast, restoration of glucose uptake under insulin-resistant conditions suggests that the extracts may selectively improve glucose utilization under pathological metabolic states, acting more as metabolic modulators rather than direct insulin mimetics. This observation is particularly relevant in the context of dexamethasone-induced insulin resistance, which is widely used as an in vitro model of type 2 diabetes due to suppression of glucose transport pathways [36]. The strong activity observed in the ZM6 water-phase crude extract is consistent with its chemical profile. GC–MS analysis identified a relatively high abundance of D-allose in this fraction, a rare sugar previously reported to be associated with modulation of glucose metabolism and insulin-related pathways [37]. This supports the possibility that D-allose may be associated with the observed improvement in glucose uptake under insulin-resistant conditions [38]. In addition, the presence of primary metabolites such as glycerol and other carbohydrate-derived compounds suggests that the observed bioactivity may not be attributable to a single compound but rather to a combined metabolic effect [39].

Although a canonical glycerol-3-phosphatase (GPP) is not explicitly annotated in the ZM4 genome, as confirmed by database analysis, the dephosphorylation of glycerol-3-phosphate may be mediated by non-specific or promiscuous phosphatase activities, as previously suggested in similar systems. This may help explain the detection of glycerol-related metabolites despite the absence of a dedicated GPP gene. These genes, as well as the Entner–Doudoroff (ED) pathway, are highly conserved in *Z. mobilis* [40, 41]. In addition, rare sugars such as D-allose are not typically encoded by dedicated biosynthetic gene clusters in bacteria; therefore, their formation may plausibly arise from promiscuous enzymatic activities within central carbon metabolism, particularly within the ED network. However, this interpretation remains speculative and requires experimental validation.

The biosynthesis of the Schiff base 2-methyl-N-(2-methylbutylidene) butan-1-amine cannot be fully explained by canonical Ehrlich pathway enzymes in *Z. mobilis*. While branched-chain aminotransferases are present, previous studies have reported that pyruvate decarboxylase (PDC: ZMO1360) exhibits limited substrate flexibility toward bulky branched keto acids. Kinetic analyses showed that wild-type PDC preferentially utilizes short-chain substrates such as pyruvate, with negligible activity toward sterically hindered 2-keto acids [42]. This suggests that aldehyde intermediates may arise through non-enzymatic reactions, such as Strecker-type degradation during fermentation or extraction, followed by spontaneous Schiff base formation. However, this remains a hypothesis and requires further validation.

In contrast, no clear genetic evidence was found supporting canonical biosynthetic routes for diketopiperazines or β-carbolines. These compounds are typically associated with cyclodipeptide synthases, non-ribosomal peptide synthetases, or tryptophan decarboxylases, none of which were detected in the ZM4 genome [43, 44]. This suggests that their formation in *Z. mobilis* may involve non-canonical, highly divergent, or currently uncharacterized biosynthetic mechanisms. Multifunctional or sequence-divergent enzymes, potentially similar to McbB-like proteins, may contribute to these transformations [45]. However, the current genomic data are insufficient to definitively assign these biosynthetic pathways. Therefore, isotopic labeling and transcriptomic approaches will be required to clarify the metabolic origins of these secondary metabolites.

Limitations

This study provides valuable insights into the antibacterial and antidiabetic potential of secondary metabolites derived from *Z. mobilis*, however, several limitations must be acknowledged. First, the biological evaluations were conducted using crude extracts and partially purified HPLC fractions rather than isolation of pure compounds. Although GC–MS tentatively identified putative bioactive molecules, such as cyclo (Pro-Leu), *β*-carbolines, and D-allose, the direct attribution of the observed bioactivities to these individual compounds remains to be experimentally validated using purified compounds or authentic standards. Second, the experimental models utilized in this study were strictly in vitro. The antibacterial effectiveness was evaluated using disk diffusion and microbroth dilution assays, and the antidiabetic potential was assessed via glucose uptake in dexamethasone-induced insulin-resistant L6 rat myotubes. While these serve as strong preliminary screening models, they do not account for the complex pharmacokinetics, bioavailability, and potential toxicity of these active metabolites within a living organism. Therefore, in vivo animal studies are required to confirm the physiological relevance, safety, and therapeutic index of these extracts. Third, the GC-MS analysis was semi-quantitative, calculating the relative abundance of metabolites based on total ion chromatograms. A targeted, fully quantitative metabolomic approach including internal standards would provide a more precise concentration profile of the active compounds. Finally, a significant barrier encountered in this study was the difference between the metabolomic profile and the *in silico* genomic predictions. Despite the detection of diketopiperazines, genomic analysis of the reference ZM4 strain failed to identify canonical biosynthetic gene clusters (BGCs), such as cyclodipeptide synthases or non-ribosomal peptide synthetases. As a result, the exact biosynthetic pathways responsible for the production of these secondary metabolites could not be fully elucidated. Future research should prioritize transcriptomic analyses, gene knockout studies, and the screening of isolated, pure compounds in in vivo models to definitively map these uncharacterized biosynthetic mechanisms and validate their clinical potential.

Conclusion

In summary, this study highlights the bioactive potential of *Zymomonas mobilis* ZM6 as a potential source of extracellular metabolites with antibacterial and antidiabetic activities. Through bioassay-guided fractionation, we demonstrated that ZM6 n-butanol extracts exhibit inhibitory activity against a range of bacterial strains, including multidrug-resistant (MDR) isolates, while the water-phase extracts, enriched in D-allose-associated fractions, enhanced glucose uptake in insulin-resistant L6 myotubes.

However, a discrepancy was observed between the bioactivity profiles and the available genomic annotations, which do not fully account for the biosynthesis of several detected metabolites. This suggests the possibility of non-canonical or currently uncharacterized metabolic pathways in *Z. mobilis*. Future studies employing stable isotope labeling (^{13}C-glucose), targeted metabolomics, and multi-omics approaches will be required to validate de novo biosynthesis and exclude potential contributions from media-derived compounds.

Overall, these findings support the potential of *Z. mobilis* as a microbial source of bioactive metabolites relevant to both metabolic regulation and antimicrobial applications.

Abbreviations

MDR
Multidrug resistance
HPLC
High performance liquid chromatography
GC-MS
Gas chromatography- mass spectrometry
ED
Entner-Doudoroff
GRAS
Generally recognized as safe
FOS
Fructooligosaccharides
ATCC
American Type Culture Collection
RM
Rich medium
OD
Optical density
CFU
Colony-forming unit
EI
Electron impact
TIC
Total ion chromatogram
DMEM
Dulbecco's Modified Eagle Medium
FBS
Fetal bovine serum
BLAST
Basic local alignment search tool
antiSMASH
Antibiotics and secondary metabolites Analysis Shell
UniProt
Universal protein resource
SD
Standard deviation
ANOVA
Analysis of variance
WP
Water-phase
BP
Butanol-phase
DKP
Diketopiperazine
NCBI
National Center for Biotechnology Information
GPP
Glycerol-3-phosphatase
CDPS
Cyclodipeptide synthases
NRPS
Non-ribosomal peptide synthetases

Declarations

Ethics approval and consent to participate

Not applicable

Consent for publication

Not applicable

Not applicable. This study did not involve human participants, human data, human tissue, or animal experiments. All experiments were performed using established *in vitro* cell lines.

Competing Interests

The authors declare that there are no conflicts of interest

Author Contribution

The study was conceptualized by YJJ and KKA. Methodology was developed by YJJ, JHY, SSC, and YTJ. Software-related analyses were performed by JSY and NKA. Investigation was carried out by KKA, JHY, SSC, NKA, and MJK. Data curation was performed by KKA, JHY, and JSY. Formal analysis was conducted by KKA, SSC, NKA, MJK, JSY, and YJJ. The original draft of the manuscript was written by KKA, JHY, and SSC. Review and editing of the manuscript were performed by YJJ, BSH, JHY, SSC, and KKA. Visualization was performed by KKA and JSY. Supervision, funding acquisition, and project administration were provided by BSH and YJJ. All authors read and approved the final manuscript.

Acknowledgement

This work was supported by the National Research Foundation of Korea (NRF) grant funded by the Korean government (MSIT) (No. 2018R1D1A1A090842), the Nakdonggang National Institute of Biological Resources (NNIBR), funded by the Ministry of Climate, Energy and Environment (MCEE) of the Republic of Korea (Grant No. NNIBR20263111), and Pukyong National University through the Industry-University Cooperation Foundation's 2025 Post-Doc Support Project and the Global Joint Research Program (No. 202506690001). In addition, the first author (KKA) acknowledges financial support from the Global Korea Scholarship (GKS) program (No. GKS-G-2020-385), funded by the Korean government, which supported their master's degree tuition.

Data Availability

The datasets used and analyzed during the current study are available from the corresponding author upon reasonable request.

References

1. Swings J, De Ley J. The biology of *Zymomonas*. Bacteriol Rev. 1977:411–46.10.1128/br. 41.1.1-46.1977.
2. Herrera CRJ, Vieira VR, Benoliel T, Carneiro CVGC, De Marco JL, de Moraes LMP, de Almeida JRM, Torres FAG. Engineering *Zymomonas mobilis* for the Production of Xylonic Acid from Sugarcane Bagasse Hydrolysate. Microorganisms. 2021:91372. 3390/microorganisms9071372.
3. Yang S, Fei Q, Zhang Y, Contreras LM, Utturkar SM, Brown SD, Himmel ME, Zhang M. *Zymomonas mobilis* as a model system for production of biofuels and biochemicals. Microb Biotechnol 2016:9699–717. 10.1111/1751-7915.12408.
4. Zhang Q, Nurhayati, Cheng CL, Lo YC, Nagarajan D, Hu J et al. Ethanol production by modified polyvinyl alcohol-immobilized *Zymomonas mobilis* and in situ membrane distillation under very high gravity conditions. Appl Energy. 2017:2021–5. 1016/. j.apenergy.2017.05.147.
5. Braga A, Gomes D, Rainha J, Amorim C, Cardoso BB, Gudiña EJ, Silvério SC, Rodrigues JL, Rodrigues LR. *Zymomonas mobilis* as an emerging biotechnological chassis for the production of industrially relevant compounds. Bioresour Bioprocess. 2021:8128. 10.1186/s40643-021-00483-2.
6. Tallyne de Aguiar Silva A, Lima Cavalcanti ID, Ayanny de Lima Fernandes M, Gisele de Oliveira Coimbra C. Manoella de Souza Lima G. Effect of *Zymomonas mobilis* probiotic on cholesterol and its lipoprotein fractions and the intestinal regulation. Clin Nutr. 2020:393750–3755. 1016/. j.clnu.2020.04.002.
7. Liu L, Li JT, Li SH, Liu LP, Wu B, Wang YW, Yang SH, Chen CH, Tan FR, He MX. The potential use of *Zymomonas mobilis* for the food industry. Crit Rev Food Sci Nutr. 2024:644134–4154. 10.1080/10408398.2022.2139221.
8. He MX, Wu B, Qin H, Ruan ZY, Tan FR, Wang JL, Shui ZX, Dai LC, Zhu QL, Pan K, Tang XY, Wang WG, Hu QC. *Zymomonas mobilis*: a novel platform for future biorefineries. Biotechnol Biofuels. 2014:7101. 10.1186/1754-6834-7-101.
9. Xia J, Liu CG, Zhao XQ, Xiao Y, Xia XX, Bai FW. Contribution of cellulose synthesis, formation of fibrils and their entanglement to the self-flocculation of *Zymomonas mobilis*. Biotechnol Bioeng. 2018:1152714–2725. 10.1002/bit.26806.
10. Todhanakasem T, Salangsing OL, Koomphongse P, Kaewket S, Kanokratana P, Champreda V. *Zymomonas mobilis* Biofilm Reactor for Ethanol Production Using Rice Straw Hydrolysate Under Continuous and Repeated Batch Processes. Front Microbiol 2019:101777. 10.3389/fmicb.2019.01777.

11. Lou J, Wang J, Yang Y, Yang Q, Li R, Hu M, He Q, Du J, Wang X, Li M, Yang S. Development and characterization of efficient xylose utilization strains of *Zymomonas mobilis*. Biotechnol Biofuels. 2021:14231. 10.1186/s13068-021-02082-x.
12. Yim JH, Kim JO, Jeon YJ. Complete genome sequence of the auto-flocculent strain *Zymomonas mobilis* ZM401. Korean J Microbiol 2021:57220–222. 10.7845/kjm.2021.1064.
13. Cao LY, Yang YF, Zhang X, Chen YH, Yao JW, Wang X, Xia J, Liu CG, Yang SH, Römling U, Bai FW. Deciphering Molecular Mechanism Underlying Self-Flocculation of *Zymomonas mobilis* for Robust Production. Appl Environ Microbiol. 2022:88e0239821. 10.1128/aem.02398-21. Epub 2022 Apr 25.
14. Liu Y, Hu L, Liu B, Qu Z. Membrane-targeting antibacterial isoniazid schiff base against *S. aureus* and biofilms. Front Chem. 2025:131654358. 10.3389/fchem.2025.1654358.
15. Haffie TL, Louie PW, Khachatourians GG. Isolation of Noninhibitory Strains of *Zymomonas mobilis*. Appl Environ Microbiol. 1985:491007–9. 10.1128/aem. 49.4.1007-1009.1985.
16. de Morais JO, Rios EM, Calazans GM, Lopes CE. *Zymomonas mobilis* research in the Pernambuco Federal University. J Biotechnol. 1993:3175–91. 10.1016/0168–1656(93)90138-d.
17. Souza LMGM, Souza LIO, Rosato YB, Araujo JM. Detection of bacteriocins in *Zymomonas mobilis* and RAPD fingerprinting of the producer strains. Afr J Pharm Pharmacol. 2011:52132–2139. 10.5897/AJPP11.328.
18. Calazans GMT, Lopes CE, Lima RMOC, de França FP. Antitumor activities of levans produced by *Zymomonas mobilis* strains. Biotechnol Lett. 1997:1919–21. 10.1023/A:1018350617120.
19. Santos Jde F, Vasconcelos J, de Souza JR, Coutinho Ede M, Montenegro SM, Azevedo-Ximenes E. The effect of *Zymomonas mobilis* culture on experimental *Schistosoma mansoni* infection. Rev Soc Bras Med Trop. 2004:37502–4. 10.1590/s0037-86822004000600015.
20. Azerêdo GA, Stamford TLM, Souza EL, Veras FF, Almeida ER, Araújo JM. In vivo assessment of possible probiotic properties of *Zymomonas mobilis* in a Wistar rat model. Electron J Biotechnol. 2010;13:3–4. 10.4067/S0717-34582010000200003.
21. Rutkis R, Ļaša Z, Rubina M, Ščerbaka R, Kalniņš G, Bogans J et al. Antimicrobial activity of *Zymomonas mobilis* is related to its aerobic catabolism and acid resistance. Fermentation. 2022:877. 10.3390/fermentation8020077.
22. Goodman AE, Rogers PL, Skotnicki ML. Minimal medium for isolation of auxotrophic *Zymomonas* mutants. Appl Environ Microbiol. 1982:44496–498. 10.1128/aem. 44.2.496-498.1982.
23. Lee M, Choi TJ. Antimicrobial Resistance Caused by KPC-2 Encoded by Promiscuous Plasmids of the Klebsiella pneumoniae ST307 Strain. Ann Lab Med. 2021;41(1):86–94. 10.3343/alm.2021.41.1.86. . Epub 2020 Aug 25.
24. Jug U, Naumoska K, Metličar V, Schink A, Makuc D, Vovk I, Plavec J, Lucas K. Interference of oleamide with analytical and bioassay results. Sci Rep. 2020:102163. 10.1038/s41598-020-59093-1.
25. Hudzicki J. Kirby-Bauer disk diffusion susceptibility test protocol. Washington (DC): American Society for Microbiology; 2009.
26. Garcia Maset R, Hapeshi A, Hall S, Dalgliesh RM, Harrison F, Perrier S. Evaluation of the Antimicrobial Activity in Host-Mimicking Media and In Vivo Toxicity of Antimicrobial Polymers as Functional Mimics of AMPs. ACS Appl Mater Interfaces. 2022:1432855–32868. 10.1021/acsami.2c05979.
27. Shahid I, Rizwan M, Mehnaz S. Identification and Quantification of Secondary Metabolites by LC-MS from Plant-associated *Pseudomonas aurantiaca* and *Pseudomonas chlororaphis*. Bio Protoc. 2018: 8e2702. 10.21769. /BioProtoc.2702.
28. Hashmi LS, Hossain MA, Weli AM, Al-Riyami Q, Al-Sabahi JN. Gas chromatography-mass spectrometry analysis of different organic crude extracts from the local medicinal plant of Thymus vulgaris L. Asian Pac J Trop Biomed. 2013:369–73. 10.1016/S2221. -1691(13)60026-X.
29. Wei CK, Tsai YH, Korinek M, Hung PH, El-Shazly M, Cheng YB, Wu YC, Hsieh TJ. Chang FR6-Paradol and 6-shogaol, the pungent compounds of ginger, promote glucose utilization in adipocytes and myotubes, and 6-paradol reduces blood glucose in high-fat diet-fed mice. Int J Mol Sci. 2017:18168. 10.3390/ijms18010168.
30. Maldoni B. Alkaloids: isolation and purification. J Chem Educ. 1991:68700. 10.1021/ed068p700.
31. Zou H, Koh JJ, Li J, Qiu S, Aung TT, Lin H, Lakshminarayanan R, Dai X, Tang C, Lim FH, Zhou L, Tan AL, Verma C, Tan DT, Chan HS, Saraswathi P, Cao D, Liu S, Beuerman RW. Design and synthesis of amphiphilic xanthone-based, membrane-targeting antimicrobials with improved membrane selectivity. J Med Chem. 2013:562359–2373. 10.1021/jm301683j.
32. Lalitha P, Veena V, Vidhyapriya P, Lakshmi P, Krishna R, Sakthivel N. Anticancer potential of pyrrole (1, 2, a) pyrazine 1, 4, dione, hexahydro 3-(2-methyl propyl) (PPDHMP) extracted from a new marine bacterium, *Staphylococcus* sp. strain MB30. Apoptosis 2016:21566–577.1007/s10495- 10. 016-1221-x.
33. Putra MY, Karim F. Antibacterial and antioxidant activity-guided isolation studies on *Fusarium* sp. associated with the ascidian *Botryllus schlosseri*. AIP Conf Proc. 2020:2243;020019. 10.1063/5.0001297.
34. Suzuki K, Nomura I, Ninomiya M, Tanaka K, Koketsu M. Synthesis and antimicrobial activity of β-carboline derivatives with N2-alkyl modifications. Bioorg Med Chem Lett. 2018:282976–2978. 10.1016/. j.bmcl.2018.06.050.
35. Beato A, Gori A, Boucherle B, Peuchmaur M, Haudecoeur R. β-Carboline as a Privileged Scaffold for Multitarget Strategies in Alzheimer's Disease Therapy. J Med Chem. 2021:641392–1422. 10.1021/acs.jmedchem.0c01887.
36. Yang Y, Wang TT, Xie HA, Hu PP, Li P. Experimental cell models of insulin resistance: overview and appraisal. Front Endocrinol (Lausanne). 2024:151469565. 10.3389/fendo.2024.1469565.
37. Ahmed A, Khan TA, Dan Ramdath D, Kendall CWC, Sievenpiper JL. Rare sugars and their health effects in humans: a systematic review and narrative synthesis of the evidence from human trials. Nutr Rev 2022:80255–270. 10.1093/nutrit/nuab012.
38. Noge S, Kumamoto K, Matsukawa H, Ando Y, Suto H, Kondo A, Kishino T, Oshima M, Suzuki Y, Okano K. Intravenous D–allose administration improves blood glucose control by maintaining insulin secretion in diabetic mice with transplanted islets. Exp Ther Med. 2025:2963. 10.3892/etm.2025.12813.

39. Ruiz-Matute AI, Hernández-Hernández O, Rodríguez-Sánchez S, Sanz ML, Martínez-Castro I. Derivatization of carbohydrates for GC and GC-MS analyses. J Chromatogr B Analyt Technol Biomed Life Sci 2011:8791226–240. 10.1016/. j.jchromb.2010.11.013.
40. Seo JS, Chong H, Park HS, Yoon KO, Jung C, Kim JJ, Hong JH, Kim H, Kim JH, Kil JI, Park CJ, Oh HM, Lee JS, Jin SJ, Um HW, Lee HJ, Oh SJ, Kim JY, Kang HL, Lee SY, Lee KJ, Kang HS. The genome sequence of the ethanologenic bacterium *Zymomonas mobilis* ZM4. Nat Biotechnol. 2005:2363–68. 10.1038/nbt1045.
41. Sootsuwan K, Thanonkeo P, Keeratirakha N, Thanonkeo S, Jaisil P, Yamada M. Sorbitol required for cell growth and ethanol production by *Zymomonas mobilis* under heat, ethanol, and osmotic stresses. Biotechnol Biofuels. 2013:6180. 10.1186/1754-6834-6-180.
42. Siegert P, McLeish MJ, Baumann M, Iding H, Kneen MM, Kenyon GL, Pohl M. Exchanging the substrate specificities of pyruvate decarboxylase from *Zymomonas mobilis* and benzoylformate decarboxylase from *Pseudomonas putida*. Protein Eng Des Sel. 2005:18345–357. 10.1093/protein/gzi035.
43. Mishra AK, Choi J, Choi SJ, Baek KH. Cyclodipeptides: An Overview of Their Biosynthesis and Biological Activity. Molecules 2017:221796. 10.3390/molecules22101796.
44. Williams BB, Van Benschoten AH, Cimermancic P, Donia MS, Zimmermann M, Taketani M, Ishihara A, Kashyap PC, Fraser JS, Fischbach MA. Discovery and characterization of gut microbiota decarboxylases that can produce the neurotransmitter tryptamine. Cell Host Microbe. 2014:16495–503. 10.1016/j.chom.2014.09.001.
45. Mori T, Hoshino S, Sahashi S, Wakimoto T, Matsui T, Morita H, Abe I. Structural basis for β-carboline alkaloid production by the microbial homodimeric enzyme McbB. Chem Biol. 2015:22898–906. 10.1016/. j.chembiol.2015.06.006.

Figures

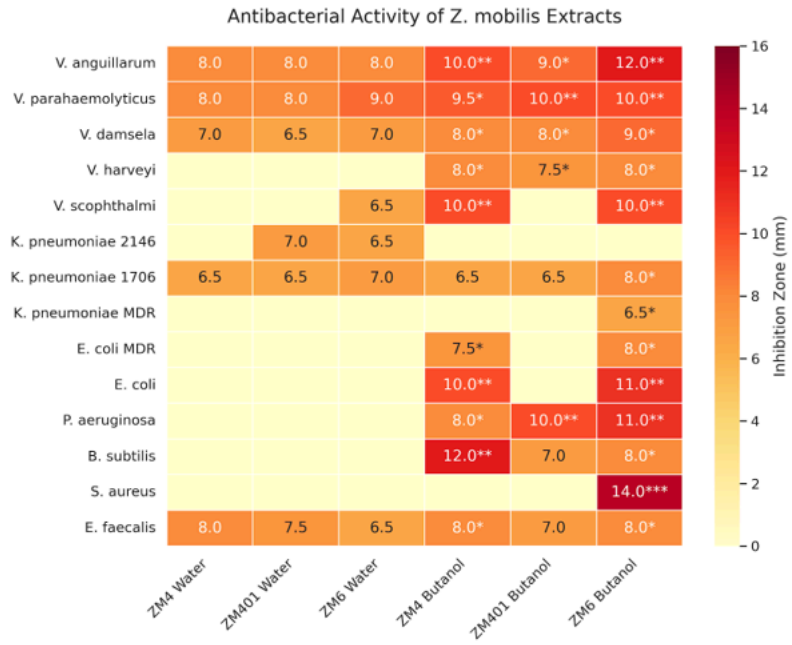


Figure 1

Heatmap of the antibacterial sensitivity profile of *Z. mobilis* crude extracts against 14 pathogenic bacteria. The heatmap displays the inhibition zone diameters (mm) produced by water phase and *n*-butanol extracts from three *Z. mobilis strains* (ZM4, ZM401, and ZM6). The color intensity represents the magnitude of the inhibition zone, with darker colors indicating higher antibacterial activity. Statistical significance compared to the negative control is denoted by asterisks within the cells: $^{*}p < 0.05$; $^{**}p < 0.01$; $^{***}p < 0.001$. Note: The positive control (enrofloxacin, 50 μg mL^{-1}) exhibited distinct inhibition zones (> 30 mm) against most tested strains; however, these data were excluded from the heatmap to optimize the visual resolution of the extract activities (6–14 mm).

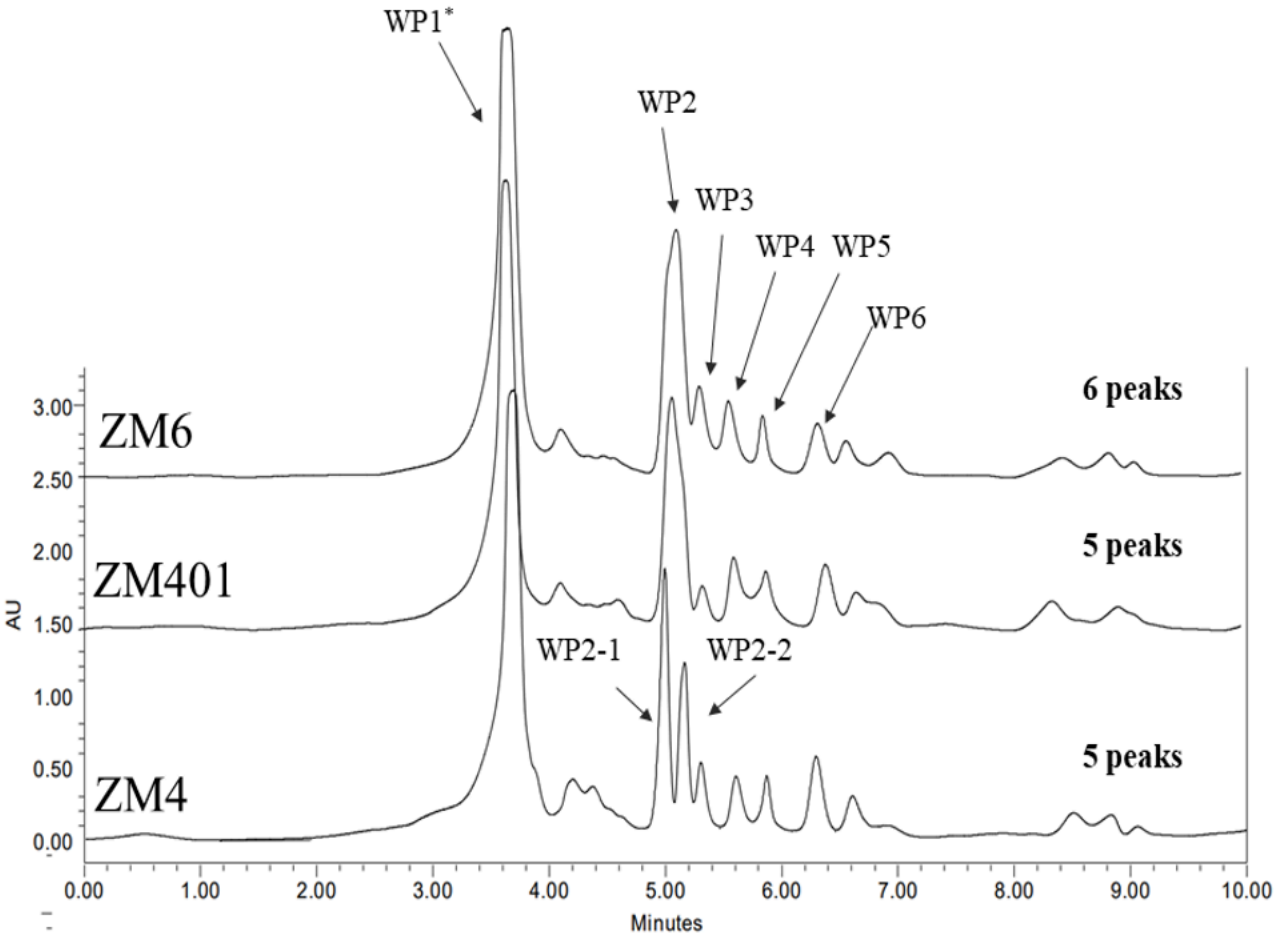


Figure 2

HPLC chromatograms of water-phase crude extracts from *Zymomonas mobilis* strains (ZM4, ZM401, and ZM6) showing peak fractionation profiles used for subsequent activity-guided analysis. Chromatograms illustrate strain-dependent differences in the number and distribution of detectable peaks withinthe polar metabolite fraction. The major peaks were collected and labeled WP1–WP6. ZM6 exhibited a higher number of resolvable peaks compared to ZM4 and ZM401, suggesting a broader diversity of polar metabolites. These fractionation profiles served as the basis for downstream antibacterial activity assays and compound identification. (*WP1: water phase peak number 1).

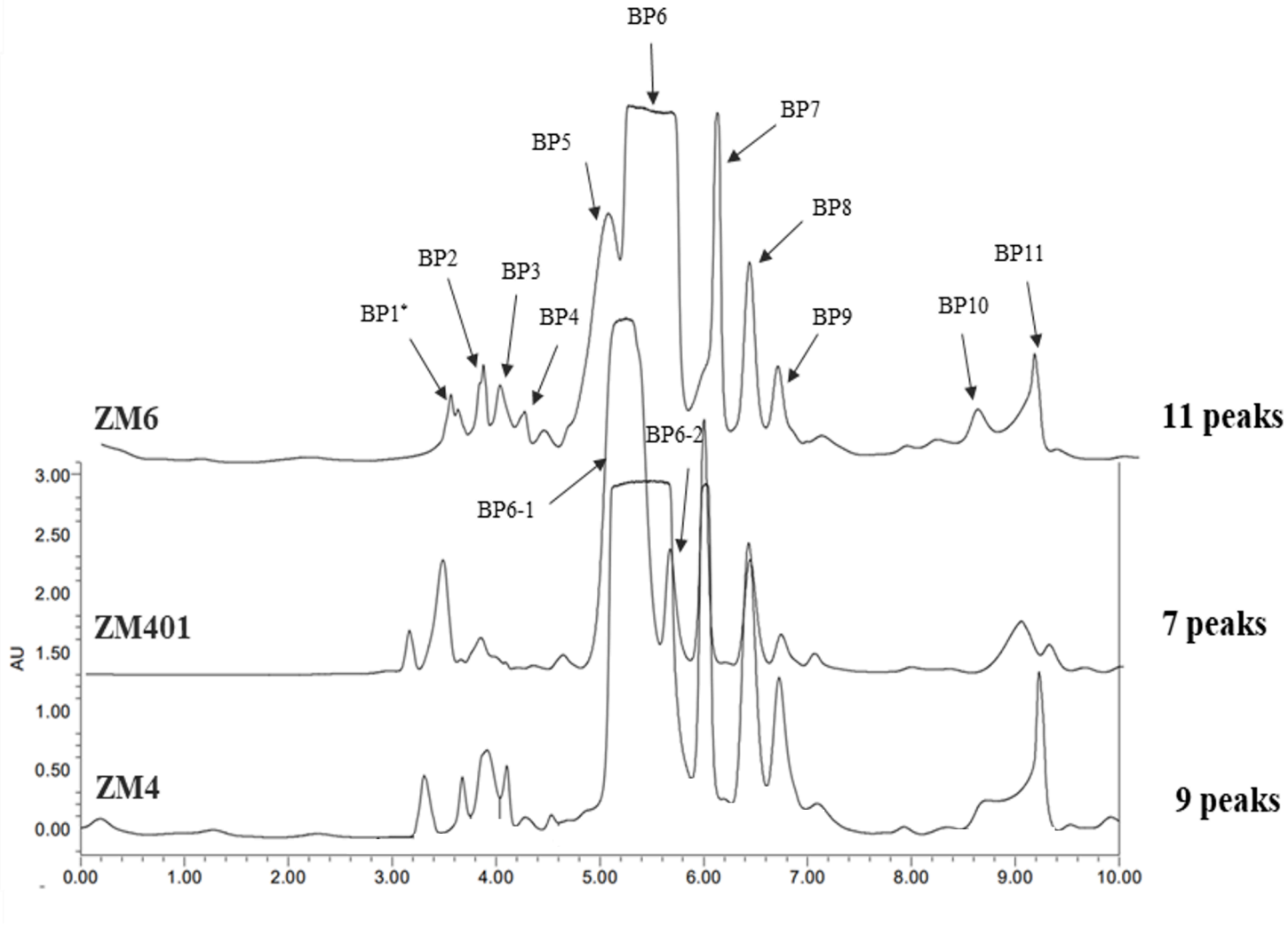


Figure 3

HPLC chromatograms of *n*-butanol phase crude extracts from *Zymomonas mobilis* strains (ZM4, ZM401, and ZM6) showing peak fractionation profiles used for downstream compound analysis. Chromatograms revealed strain-dependent differences in the number and distribution of peaks within the *n*-butanol extract, with ZM6 exhibiting the highest number of resolvable peaks (BP1–BP11), followed by ZM401 (9 peaks) and ZM4 (7 peaks). Labeled peaks indicate fractions collected for subsequent compound identification and the literature-based evaluation of potential antibacterial relevance (Table 3). (*BP1: *n*-butanol phasepeak number 1).

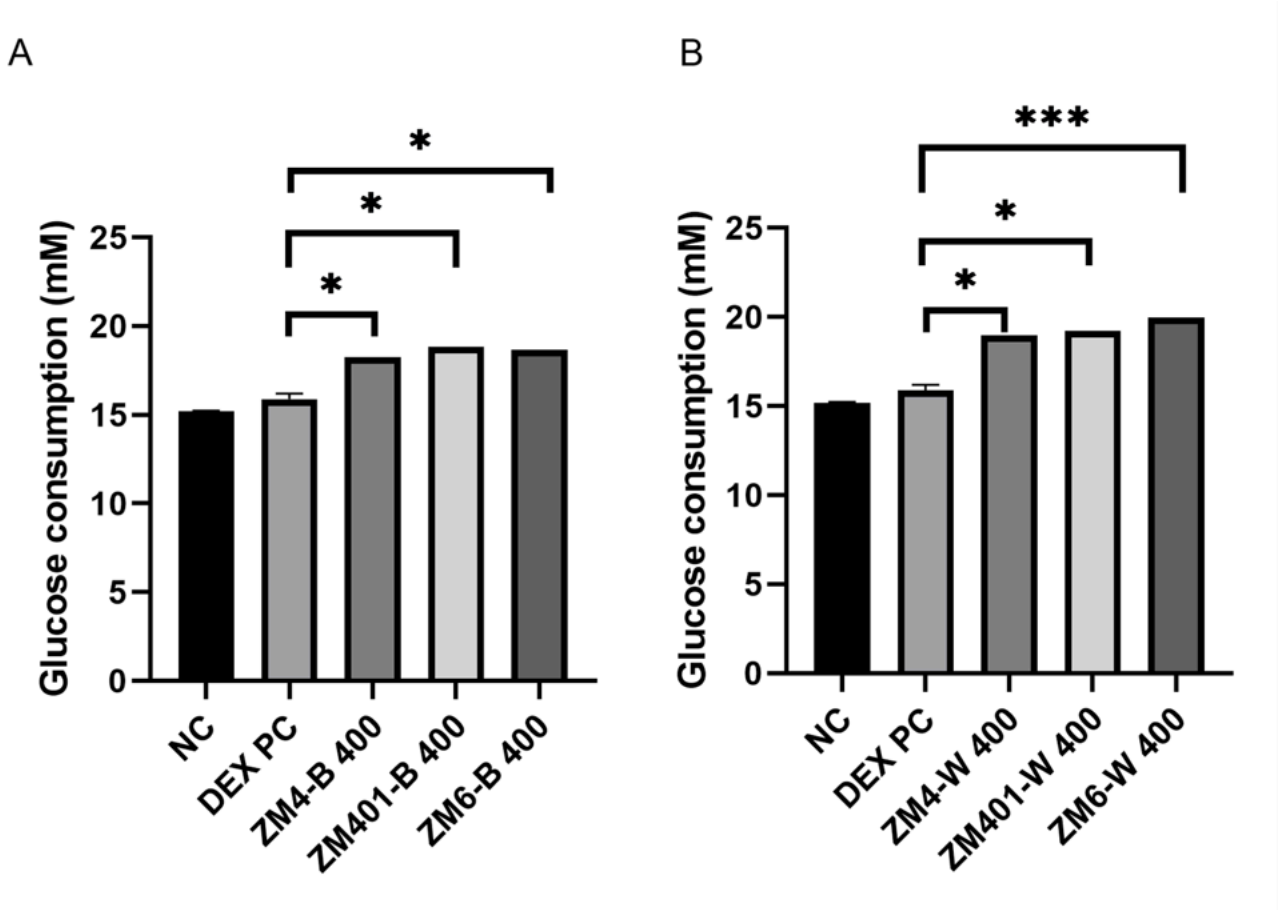


Figure 4

Antidiabetic activity of *Z. mobilis* crude extracts on glucose consumption in dexamethasone-induced insulin-resistant L6 rat myotubes. (A) Glucose consumption following treatment with n-butanol extracts (ZM4-B, ZM401-B, and ZM6-B) at a concentration of 400 µg mL^{-1}. **(B)** Glucose consumption following treatment with water-phase crude extracts (ZM4-W, ZM401-W, and ZM6-W) at a concentration of 400 µg mL^{-1}. NC represents the normal basal control, and DEX PC represents the dexamethasone-induced insulin-resistant control. Data are presented as mean ± SD. Significance level: * $p < 0.05$; *** $p < 0.001$ vs. DEX PC control.

Supplementary Files

This is a list of supplementary files associated with this preprint. Click to download.

- MetabolomicProfilingandIdentificationofBioactiveCompoundsfromZymomonasmobilisExhibitingAntibacterialandAntidiabeticPropertiesSupplementary2.
- Graphicalabstract.docx